A threading receptor for polysaccharides

Tiddo J. Mooibroek, Juan M. Casas-Solvas, Robert L. Harniman, Charles M. Renney, Tom S. Carter, Matthew P. Crump & Anthony P. Davis

Abstract

Cellulose, chitin and related polysaccharides are key renewable sources of organic molecules and materials. However, poor solubility tends to hamper their exploitation. Synthetic receptors could aid dissolution provided they are capable of cooperative action, for example by multiple threading on a single polysaccharide molecule. Here we report a synthetic receptor designed to form threaded complexes (polypseudorotaxanes) with these natural polymers. The receptor binds fragments of the polysaccharides in aqueous solution with high affinities (K_a up to 19,000 M^{-1}), and is shown—by nuclear Overhauser effect spectroscopy—to adopt the threading geometry. Evidence from induced circular dichroism and atomic force microscopy implies that the receptor also forms polypseudorotaxanes with cellulose and its polycationic analogue chitosan. The results hold promise for polysaccharide solubilization under mild conditions, as well as for new approaches to the design of biologically active molecules.

Main

Polysaccharides are the dominant organic molecules in the biosphere[1], and thus key renewable resources[2,3]. However, the most abundant, including cellulose and chitin, are generally the most difficult to utilize because of their extreme insolubility. At present no method is available to mobilize these materials in water under mild conditions, and so modifications typically involve chemical transformations in aggressive media[4,5,6] or the slow action of enzymes on undissolved solids[7]. Dissolution in aqueous media at a biological pH would allow new paths to exploitation. In particular, the polysaccharides could be exposed to enzymes, either natural or engineered, to which they would be far more vulnerable. The rapid conversion of cellulose into glucose is just one prospective outcome.

Here we adumbrate a strategy for the dissolution of cellulose, and related polysaccharides, through the application of synthetic receptors. The approach employs cage molecules with amphiphilic interiors, complementary to the carbohydrate targets. Critically, the receptors are able to thread onto the polysaccharides to form polypseudorotaxanes[8,9]. Owing to the threaded topology, many receptor molecules can bind to one polysaccharide chain and surround the polymer with hydrophilic groups. If binding is sufficiently strong to counteract the crystal-packing forces, dissolution should be feasible. We report the design and synthesis of a threading receptor for polysaccharides, and show that it forms pseudorotaxanes with water-soluble oligosaccharides. We also describe evidence for polypseudorotaxane formation from polysaccharides under certain conditions. The results demonstrate the feasibility of polysaccharide threading in water, and could point the way to systems capable of solubilization.

A defining feature of cellulose (**1**) and chitin (**2**) (Fig. 1a) is the all-equatorial disposition of intrachain linkages and polar substituents and (consequently) the axial positioning of apolar CH groups. In the extended conformation of the polymer, this creates two parallel strips of hydrophobic surfaces separated by lines of hydrogen-bonding functional groups. Our strategy to complement these supramolecular valencies is illustrated in Fig. 1b. We sought a cage-like receptor structure in which two aromatic surfaces would be held parallel to each other, and separated by rigid polar spacers. The portals of the cage would be large enough to allow threading by the polysaccharide substrates. The aromatic surfaces would be capable of forming hydrophobic and CH-π interactions with axial CH groups in the substrates, and the polar groups would hydrogen bond to equatorial substituents.

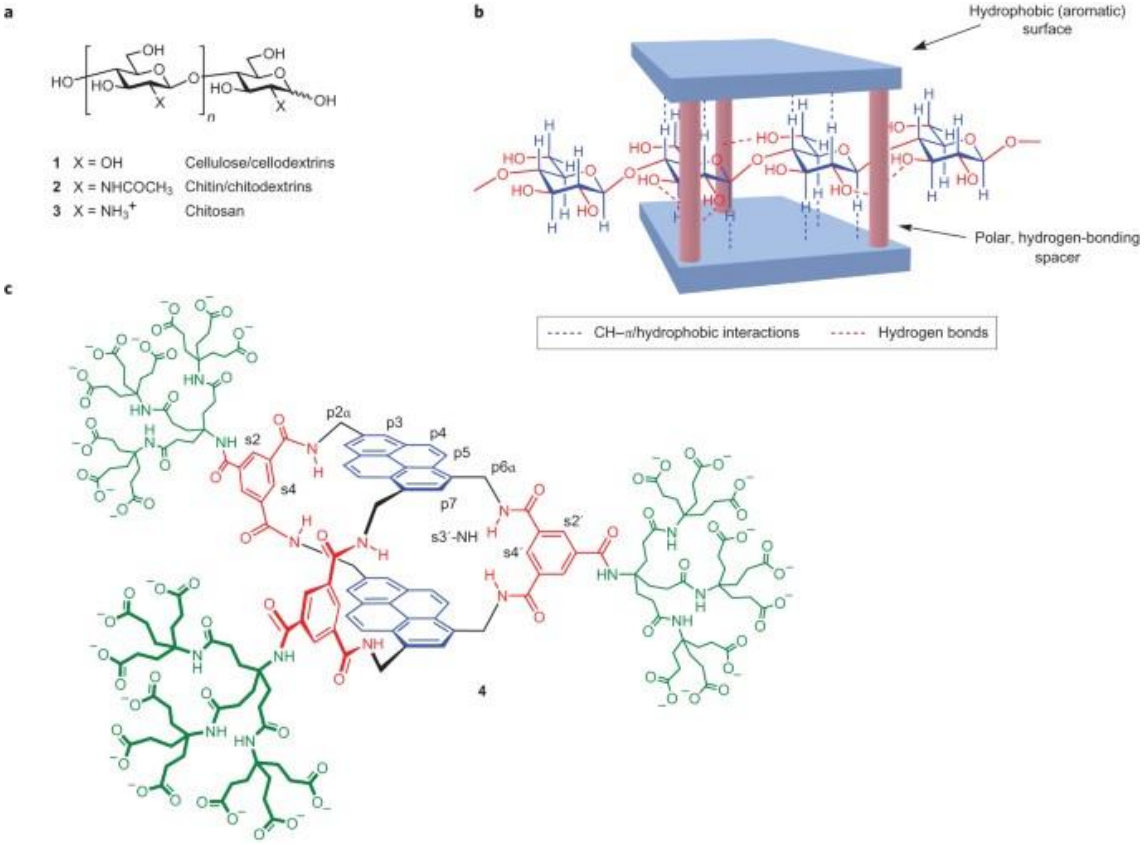

Figure 1: Receptor design. a, The all-equatorial oligo- and polysaccharide targets. **b**, Schematic design strategy, with cellulose depicted as the substrate. **c**, Polysaccharide receptor **4**, with labels for selected carbons. The complete labelling system is given in Supplementary Fig. 1. For **b** and **c**, the hydrophobic and polar moieties in the receptor core are shown in blue and red, respectively.

We had previously used a related approach to bind all-equatorial mono- and disaccharides in water[10,11,12,13]. However, these earlier designs employed flexible biphenyl[10,11] or terphenyl[12,13] units as aromatic surfaces, and required four or five spacers to maintain the preorganized cavities. The resulting cage structures were successful but size specific; they encapsulated their targets, did not allow threading and could not be applied to polysaccharides. The challenge here was to create a maintained cavity using fewer spacers and a more open architecture. Our proposed solution was to

exploit condensed aromatic units as extended rigid hydrophobic surfaces. Specifically, the tetracyclic pyrene possesses a surface that easily spans a monosaccharide residue. Two pyrene units and three isophthalamide spacers may be combined to form the symmetrical bicyclic structure **4** (Fig. 1c). Molecular modelling predicted that **4** would retain an open structure in water, despite the potential for hydrophobically driven collapse, and that a cellulose chain could, indeed, pass through the larger portals of the cavity while hydrogen bonding to annular amides in the spacers (see Fig. 1b, and also Fig. 2d). The design also incorporates three externally directed dendrimeric nonacarboxylate units to ensure water solubility[14,15].

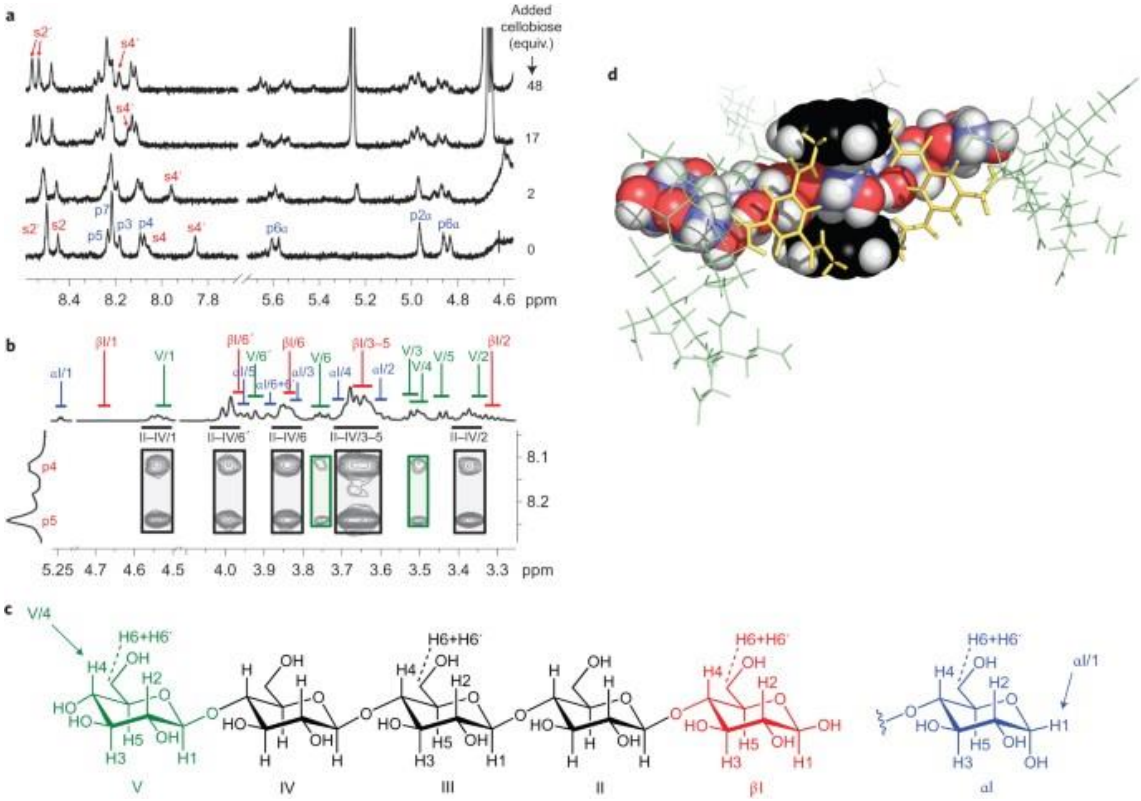

Figure 2: ^{1}H NMR evidence for receptor 4 binding oligosaccharides. a, Partial spectra (500 MHz) from a titration of **4** (0.5 mM) against D-cellobiose (**1**, *n* = 1) in D_2O at 80 °C (see Fig. 1 for the proton numbering). **b**,**c**, Partial NOESY spectrum (D_2O, 600 MHz) of **4** (0.25 mM) + D-cellopentaose **1** (*n* = 4) (4.7 mM), with the assignments (**b**) and the labelling key (**c**). The cross-peaks to internal saccharide residues II–IV (in the black rectangles) dominate the spectrum. **d**, Calculated structure of **4** + **1** (*n* = 4) consistent with the NOESY spectrum. The pyrene units and cellopentaose are shown in a space-filling mode: yellow, isophthalamide spacers; green, side-chains; black, pyrenyl carbon; blue, carbohydrate carbon; red, oxygen; white, hydrogen. The conformation was energy-minimized using MacroModel 10.3 (Maestro 9.7 interface) with the Merck Molecular Force Field (static) and Generalized Born/Surface Area (water) continuum solvation.

Results and discussion

Receptor **4** was synthesized from pyrene via pyrene-2-carboxylic acid16 as described in Supplementary Section 1. Solutions of **4** in water at pH = 7 and 25 °C gave moderately resolved ^{1}H NMR spectra that did not change significantly between 1 mM and 5 μM, which implies the receptor was monomeric over this range of concentrations (see Supplementary Fig. 2). On warming to 80 °C the resolution improved, consistent with conformational mobility, which is fast at the higher temperature but slow enough to cause signal broadening at 25 °C (see Supplementary Fig. 3). Possible motions are rotations of the annular amide groups between 'NH-in' orientations, as shown in Fig. 1, and 'NH-out' in which the amide carbonyl points inwards. Evidence for such movements was provided by nuclear Overhauser effect spectroscopy (NOESY) connections between the amide protons and spacer aromatic CH groups. For example, the integration of NOESY cross-peaks between s3'-NH and the inward-directed s4', as against the outward-directed s2', implied that this NH is 87% 'NH-in' and 13% 'NH-out' at 25 °C. The equilibrium position was found to be temperature dependent; the 'NH-in' conformation predominates by 81 and 93% at 5 and 80 °C, respectively (see Supplementary Figs 4–7).

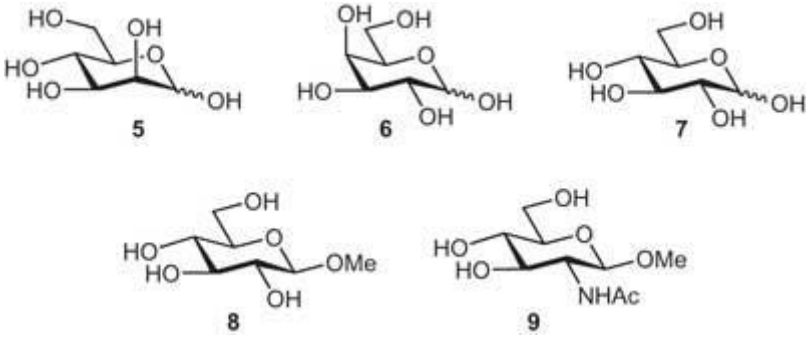

The binding properties of **4** were studied using ^{1}H NMR titrations and isothermal titration calorimetry (ITC) in aqueous solution (the details are given in Supplementary Section 2). Monosaccharides **5**–**9** and a series of all-equatorial oligosaccharides (see Table 1) were used as substrates. In most cases, the addition of carbohydrate to **4** caused movements of the receptor ^{1}H NMR signals, consistent with complex formation that is fast on the NMR timescale. The changes are illustrated in Fig. 2a for **4** + cellobiose; these spectra were acquired at 80 °C to reduce signal broadening, but similar movements could be observed and followed at 25 °C. The splitting of some receptor signals (for example, s2') is consistent with a C_{2v} receptor such as **4** in a fast exchange with an asymmetrical substrate (for clarification, see Supplementary Fig. 8). For the monosaccharides, and also for chitobiose (**3**, n = 1), affinities could be quantified by nonlinear least-squares curve fitting of the NMR signal movements assuming a 1:1 binding model. Supporting values for methyl glucoside (**8**) and methyl *N*-acetyl-β-D-glucosaminide (GlcNAc-β-OMe) (**9**) could be obtained from ITC. For the cellodextrins (**1**), the NMR plots showed signs that further substrate molecules could bind weakly to the initial 1:1 complex (see Supplementary Figs 14 and 15). However, ITC gave plots which fit well to a 1:1 binding model (see Fig. 3 and Supplementary Figs 17–23). As weak secondary binding is unlikely to interfere with ITC analysis (because of the small thermal signal), the derived association constants were considered reliable. ITC was also employed for chitodextrins (**2**) (see Supplementary Figs 24 and 25), as NMR titrations gave signal broadening. The results from both NMR and ITC are summarized in Table 1; when both methods could be used they showed good agreement.

Table 1 K_a and thermodynamic parameters for receptor 4 binding carbohydrates in H_2O/D_2O at 298 K.

Carbohydrate	K_a NMR/ITC (M^{-1})	ΔG^*	ΔH^*	$T\Delta S^*$
		(kJ mol^{-1})		
D-Mannose (5)	~5/n.d.[†]	–	–	–
D-Galactose (6)	18/n.d.[†]	–	–	–
D-Glucose (7)	120/n.d.[†]	–	–	–
Methyl β-D-glucoside (8)	240/260	−13.7	−7.2	6.6
GlcNAc-β-OMe (9)	270/190	−13.0	−6.4	6.7
D-Cellobiose (**1**, *n* = 1)	3,900[‡]/3,600	−20.3	−8.9	11.4
D-Cellotriose (**1**, *n* = 2)	5,200[‡]/5,000	−21.1	−8.0	13.1
D-Cellotetraose (**1**, *n* = 3)	n.d.[†]/12,000	−23.3	−7.6	15.7
D-Cellopentaose (**1**, *n* = 4)	n.d.[†]/8,800	−22.5	−8.8	13.7
D-Cellohexaose (**1**, *n* = 5)	n.d.[†]/8,700	−22.5	−8.7	13.8
N,*N*'-diacetyl-D-chitobiose (**2**, *n* = 1)	n.d.[†]/2,200	−19.1	−10.1	9.0
N,*N*',*N*''-triacetyl-D-chitotriose (**2**, *n* = 2)	n.d.[†]/2,400	−13.0	−6.4	6.7
D-Chitobiose (**3**, *n* = 1)[§]	19,000/n.d.[†]	–	–	–

*From ITC. [†]Not determined. [‡]K_a for 1:1 binding. Analysis suggests weak binding of a second substrate molecule with K_a = 33 M^{-1} (cellobiose) and 39 M^{-1} (cellotriose). [§]pH = 7.

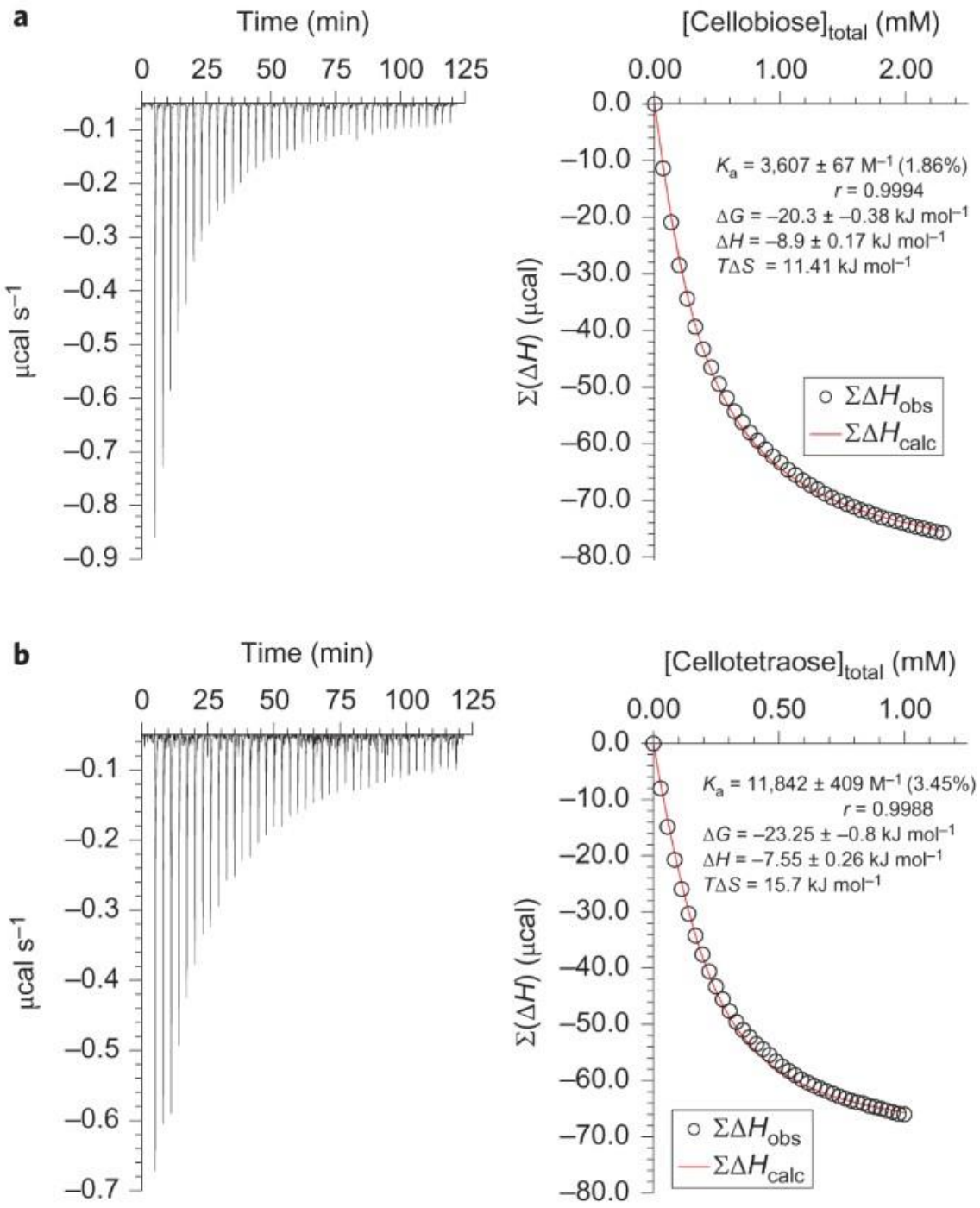

Figure 3: Representative ITC data and analysis curves. a, Addition of cellobiose (**1**, n = 1) (13.05 mM) to **4** (0.2 mM, 200 µl) in water; K_a = 3,600 M^{-1}. **b**, Addition of cellotetraose (**1**, n = 3) (5.66 mM) to **4** (0.2 mM, 200 µl) in water; K_a = 12,000 M^{-1}. calc, calculated; obs, observed.

The results in Table 1 show that, as expected, receptor **4** is selective for all-equatorial carbohydrates, and favours glucose (**7**) and glucoside (**8**) over mannose (**5**) or galactose (**6**). Although the binding constants for **7**, **8** and cellobiose are slightly higher than the best previously reported from our laboratory[11,17], the performance with the higher cellodextrins is outstanding. In contrast to previous systems, which showed almost no affinity for these substrates[9,11], receptor **4** binds **1** (n = 2–5) with K_a = 5,000 M^{-1} or greater. The binding constant for cellotetraose, at ~12,000 M^{-1}, is the highest observed for the

biomimetic recognition of a neutral saccharide in water. Although the affinities seem to peak at cellotetraose, there is no sign of an upper limit for the length of substrate. It is interesting that variations within the cellodextrin series are determined more by entropy (*S*) than enthalpy (*H*). It is understandable that the enthalpies for **1** (*n* = 1–5) should be roughly similar, as the interactions made and broken during binding should be nearly the same. It is also reasonable that the entropy of binding should become more favourable in the series cellobiose → cellotriose → cellotetraose (**1**, *n* = 1–3). As the substrate becomes longer it gains freedom of movement in the complex, and thus gains translational entropy. It is less obvious why the entropy of binding should peak at cellotetraose (**1**, *n* = 3), but this might relate to contacts between substrate and side chains, which could restrict the motion of both. This is consistent with the modelling. For complexes with cellobiose through to cellotetraose the receptor side chains appear largely unconstrained. However, for cellopentaose and longer substrates, the polysaccharide chain begins to clash with the side chains at the more crowded 'double-spacer' end of the receptor.

The binding constant to cationic chitobiose (**3**, *n* = 1) is even higher than that for cellotetraose, although this is unsurprising considering the charge complementarity between receptor and substrate. Acetylated chitodextrins (**2**, *n* = 1,2) were bound less strongly but still substantially. Although the affinities to **4** might seem moderate by general biological standards, they are good given that carbohydrates in water are challenging targets[18]. The values measured are well within the range observed for lectins, the major class of carbohydrate-binding proteins[19].

To confirm that **4** could thread fully onto oligosaccharides, rather than stay at one end, we performed a NOESY-based structural investigation on the complex between **4** and cellopentaose (**1**, *n* = 4). In the ^{1}H NMR spectrum of cellopentaose, it is possible to differentiate between internal residues II–IV and terminal residues I and V (see Fig. 2b)[20,21]. In the NOESY spectrum of **4** with cellopentaose, strong cross-peaks were observed from the pyrenyl protons p4/p5 to internal residues II–IV, very weak signals to the non-reducing terminus V and none to the reducing terminus I (Fig. 2b,c). Even allowing for the threefold near degeneracy of the internal residue signals, the results imply that the receptor spends most of its time in the middle of the pentasaccharide (Fig. 2d). Spectra of **4** with cellobiose and cellotriose supported this interpretation (see Supplementary Fig. 34).

With the threading geometry for oligosaccharide binding confirmed, we investigated whether **4** could form polypseudorotaxanes with all-equatorial polysaccharides. To study cellulose + **4** we dissolved the polysaccharide and receptor in 1 M NaOH (ref. 22). Previous experiments had shown that the receptor is stable to a strong aqueous base (which was used in the final deprotection step in the synthesis). Induced circular dichroism (ICD) was observed across the absorbance range of the pyrene units in the receptor (see Supplementary Fig. 36), which implies close contact between the cellulose (which may be partially deprotonated) and some molecules of the receptor[11,12]. Given the NMR evidence for cellodextrin threading, and the literature precedent for polypseudorotaxanes[9], it seems reasonable to infer the formation of multiply threaded complexes. Dilution (by 2.5 × 10^{5}) of such solutions with water, followed by deposition on mica and washing with water, gave samples suitable for study by atomic force microscopy (AFM). A typical AFM image is shown in Fig. 4a. The principle large-scale feature is a long strand that is ~1 nm broad in some regions and ~2 nm in others. This is consistent with

cellulose molecules that pair and overlap over part of their lengths. Along the feature (in particular, along the narrower parts), higher and wider bulb-like protrusions are present. The average dimensions of 34 of these protrusions were determined as 1.14 ± 0.17 nm high and 2.9 ± 0.90 nm wide. Both are consistent with the dimensions estimated for individual receptor molecules (see Supplementary Fig. 37), and the image thus seems to indicate the threading of multiple receptors onto the cellulose. The alternative arrangement, in which receptor molecules lie on top of the cellulose, should give protrusions ≥1.6 nm in height. The population of threaded receptors cannot be related to an equilibrium in solution, because the sample underwent major changes in conditions (high concentrations and pH, dilution and then returning to high concentrations on evaporation). Moreover, the experiment does not show that receptor **4** itself can solubilize cellulose at a moderate pH. However, it does seem to provide the first evidence of a polysaccharide-based polypseudorotaxane architecture. Control samples prepared from cellulose alone showed compact features that appeared to consist of multiple intertwined cellulose molecules (see Fig. 4b). This suggests that, unsurprisingly, polypseudorotaxane formation affects cellulose folding and promotes extended rather than coiled conformations. Further details and discussion of the AFM measurements are presented in Supplementary Section 5.

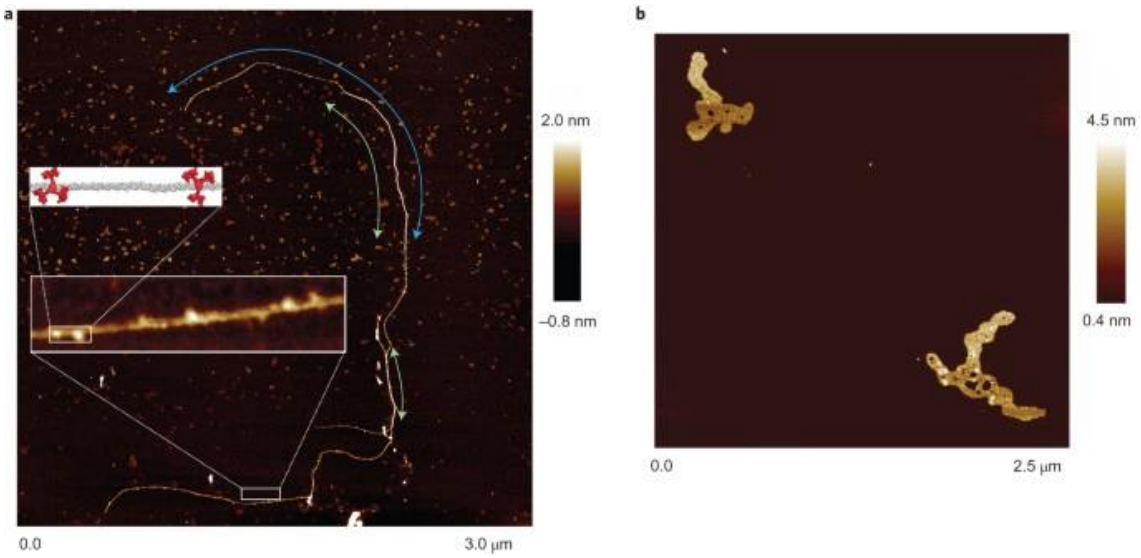

Figure 4: AFM studies of receptor 4 + cellulose. a, Image of cellulose (**1**) (100 nM glucosyl) + receptor **4** (1 nM) deposited from aqueous base. Green arrows show regions consistent with cellulose-strand pairing, and the blue arrow highlights a single cellulose molecule. Insets: a segment containing ~500 glucose monomers that show protrusions consistent with the threaded receptor **4**, and a model of part of this segment containing 40 glucose units (grey) and two receptors (red). The model is energy-minimized as for Fig. 2d, and accurately scaled. **b**, Control sample of cellulose, prepared as for **a** but without the receptor.

Studies were also performed with chitosan (**3**, n = 375–750), which is soluble under mildly acidic conditions (pH ≈ 6). Mixtures of chitosan and **4** were found to give clear solutions across the pH range 1–11. As chitosan is insoluble at a basic pH, and receptor **4** is insoluble in acid, this implied mutual solubilization. Moreover, the interaction does not seem to depend on electrostatic forces, as one component should be electrically neutral at either end of the range. It thus seems that the solubilization is not the result of chitosan

binding to the side chains of the receptor, but rather that of some other interaction geometry, most obviously threading to form polypseudorotaxanes. In support of this interpretation, several ICD bands were observed for chitosan + **4** at pH = 6.4 (see Supplementary Fig. 36). The chitosan + **4** mixture was further studied by AFM. A solution of chitosan + **4** at pH = 1 was diluted with water by 2.5 × 10^7 and then deposited on mica. AFM imaging revealed elongated plate-like structures, as illustrated in Fig. 5a and Supplementary Fig. 44. Height profiles taken along the short axis of the structures gave an average value of ~1.3 nm, with variations that suggest an underlying periodicity (a 3.5–3.8 nm lateral repeat unit (see Fig. 5b)). The data are consistent with bundles of aligned polypseudorotaxanes, one unit thick, cemented by hydrogen bonding between receptor carboxyl groups. A computational model of this arrangement (see Fig. 5a) featured interchain distances of ~3.6 nm, consistent with the AFM data. Although the chitosan cannot be detected directly in the image, its presence can be inferred from the organization imposed on the assemblies. Also, the lengths of the aggregates, at ~200–500 nm, are consistent with the estimated length range of the chitosan (188–375 nm). Control samples prepared from chitosan alone showed mainly coiled structures (see Fig. 5c and Supplementary Fig. 42), whereas receptor **4** alone, deposited from acid, gave irregular particles with widely varying sizes (see, for example, Fig. 5d). As argued for **4** + cellulose, the alternative arrangement, in which the receptor molecules stack on chitosan, should result in measured heights of ≥1.6 nm, and is therefore inconsistent with the AFM data (for further details and discussion of the AFM measurements, see Supplementary Section 5). The formation of multistrand polypseudorotaxane assemblies with closely packed macrocycles finds precedent in the well-known complexes of poly(ethylene glycol)s with α-cyclodextrin9.

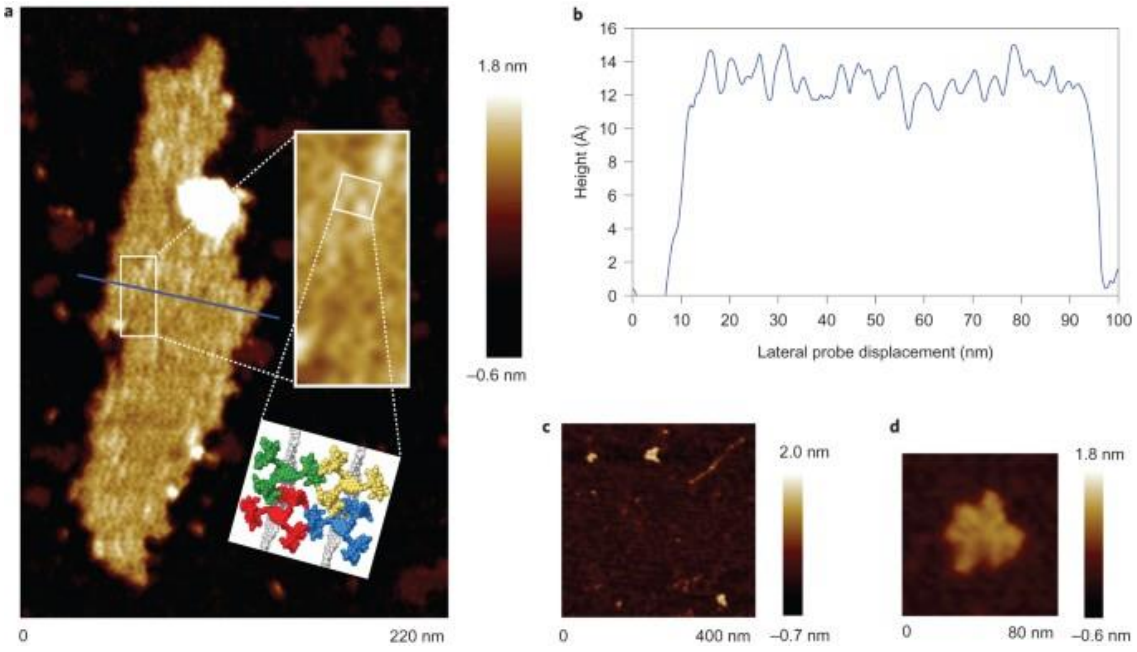

Figure 5: AFM studies of receptor 4 + chitosan. a, Image of chitosan (**3**, *n* = 375–750) (1 nM glucosaminyl) + receptor **4** (0.01 nM) deposited from aqueous acid. Chitosan and the receptor were mixed at pH = 1 and then diluted with water by 2.5 × 10^7 to obtain the final concentrations. Insets: a region of the image magnified, and a modelled portion of the proposed structure constructed from two chitosan chains (grey) and four receptors (red, green, blue and yellow). The model is energy-minimized as for Fig. 2d, and accurately

scaled. **b**, Height profile taken across the short axis of the aggregate (blue line in **a**). The variations are consistent with long-range order, as expected for molecular chains ~3.4 nm in width that lie parallel to each other. The same periodicity was observed throughout the aggregate (see Supplementary Fig. 46). **c**, Chitosan deposited from aqueous acid following the procedure used for **4** + chitosan. The compact objects suggest that most molecules adopt a coiled structure. A single extended strand was also observed (top right). **d**, Receptor **4** deposited from aqueous acid following the same procedure. Irregular aggregates are observed, up to 8 nm in height.

Conclusion

We show here that receptor **4** can form threaded complexes with oligo/polysaccharides, with affinities rising above 10^4 M^{-1}. The solubilization of cellulose or chitin through polypseudorotaxane formation will probably require yet stronger binding to overcome the forces between polysaccharide chains. However, this should be achievable by expanding the hydrophobic surfaces and supplementing the polar interactions. At present, soluble polysaccharides, such as chitosan, are already important for tissue engineering[23,24], and their applications may multiply in future. Polypseudorotaxane formation could provide a novel way to moderate their properties. Also, the biological importance of cellulose, chitin and so on suggests new modes of biological activity. For example, chitin is a major component of fungal cell walls, and a target for plant defence proteins[25]. Threading onto nascent chitin chains could provide a promising approach to antifungal agents. Finally, although threaded molecular architectures have attracted intense interest in recent years[26,27], we believe that these are the first to be formed from a synthetic receptor with biopolymers under biological (that is, aqueous) conditions. They are therefore the first with the potential for direct exploitation in biochemistry or chemical biology.

References

1. Voet, D. & Voet, J. G. *Biochemistry* (Wiley, 1995).
2. Klemm, D. et al. Nanocelluloses: a new family of nature-based materials. *Angew. Chem. Int. Ed.* **50**, 5438–5466 (2011).
3. Klemm, D., Heublein, B., Fink, H. P. & Bohn, A. Cellulose: fascinating biopolymer and sustainable raw material. *Angew. Chem. Int. Ed.* **44**, 3358–3393 (2005).
4. Heinze, T. & Liebert, T. Unconventional methods in cellulose functionalization. *Prog. Polym. Sci.* **26**, 1689–1762 (2001).
5. Zhou, C. H., Xia, X., Lin, C. X., Tong, D. S. & Beltramini, J. Catalytic conversion of lignocellulosic biomass to fine chemicals and fuels. *Chem. Soc. Rev.* **40**, 5588–5617 (2011).
6. Pinkert, A., Marsh, K. N., Pang, S. S. & Staiger, M. P. Ionic liquids and their interaction with cellulose. *Chem. Rev.* **109**, 6712–6728 (2009).
7. Brunecky, R. et al. Revealing nature's cellulase diversity: the digestion mechanism of *Caldicellulosiruptor bescii* CelA. *Science* **342**, 1513–1516 (2013).
8. Raymo, F. M. & Stoddart, J. F. Interlocked macromolecules. *Chem. Rev.* **99**, 1643–1663 (1999).

9. Harada, A., Hashidzume, A., Yamaguchi, H. & Takashima, Y. Polymeric rotaxanes. *Chem. Rev.* **109**, 5974–6023 (2009).

10. Barwell, N. P., Crump, M. P. & Davis, A. P. A synthetic lectin for beta-glucosyl. *Angew. Chem. Int. Ed.* **48**, 7673–7676 (2009).

11. Ferrand, Y. et al. A synthetic lectin for O-linked beta-*N*-acetylglucosamine. *Angew. Chem. Int. Ed.* **48**, 1775–1779 (2009).

12. Ferrand, Y., Crump, M. P. & Davis, A. P. A synthetic lectin analog for biomimetic disaccharide recognition. *Science* **318**, 619–622 (2007).

13. Sookcharoenpinyo, B. et al. High-affinity disaccharide binding by tricyclic synthetic lectins. *Angew. Chem. Int. Ed.* **51**, 4586–4590 (2012).

14. Newkome, G. R. & Shreiner, C. Dendrimers derived from 1 → 3 branching motifs. *Chem. Rev.* **110**, 6338–6442 (2010).

15. Diederich, F. & Felber, B. Supramolecular chemistry of dendrimers with functional cores. *Proc. Natl Acad. Sci. USA* **99**, 4778–4781 (2002).

16. Casas-Solvas, J. M., Mooibroek, T. J., Sandramurthy, S., Howgego, J. D. & Davis, A. P. A practical, large-scale synthesis of pyrene-2-carboxylic acid. *Synlett* **25**, 2591–2594 (2014).

17. Destecroix, H. et al. Affinity enhancements by dendritic side-chains in synthetic carbohydrate receptors. *Angew. Chem. Int. Ed.* **54**, 2057–2061 (2015).

18. Ambrosi, M., Cameron, N. R. & Davis, B. G. Lectins: tools for the molecular understanding of the glycocode. *Org. Biomol. Chem.* **3**, 1593–1608 (2005).

19. Toone, E. J. Structure and energetics of protein–carbohydrate complexes. *Curr. Opin. Struct. Biol.* **4**, 719–728 (1994).

20. Flugge, L. A., Blank, J. T. & Petillo, P. A. Isolation, modification, and NMR assignments of a series of cellulose oligomers. *J. Am. Chem. Soc.* **121**, 7228–7238 (1999).

21. Roslund, M. U., Tahtinen, P., Niemitz, M. & Sjoholm, R. Complete assignments of the H-1 and C-13 chemical shifts and J(H,H) coupling constants in NMR spectra of D-glucopyranose and all D-glucopyranosyl-D-glucopyranosides. *Carbohydr. Res.* **343**, 101–112 (2008).

22. Isogai, A. & Atalla, R. H. Dissolution of cellulose in aqueous NaOH solutions. *Cellulose* **5**, 309–319 (1998).

23. Kumar, M., Muzzarelli, R. A. A., Muzzarelli, C., Sashiwa, H. & Domb, A. J. Chitosan chemistry and pharmaceutical perspectives. *Chem. Rev.* **104**, 6017–6084 (2004).

24. Kharkar, P. M., Kiick, K. L. & Kloxin, A. M. Designing degradable hydrogels for orthogonal control of cell microenvironments. *Chem. Soc. Rev.* **42**, 7335–7372 (2013).

25. Theis, T. & Stahl, U. Antifungal proteins: targets, mechanisms and prospective applications. *Cell. Mol. Life Sci.* **61**, 437–455 (2004).

26. Balzani, V., Credi, A., Raymo, F. M. & Stoddart, J. F. Artificial molecular machines. *Angew. Chem. Int. Ed.* **39**, 3349–3391 (2000).

27. Kay, E. R., Leigh, D. A. & Zerbetto, F. Synthetic molecular motors and mechanical machines. *Angew. Chem. Int. Ed.* **46**, 72–191 (2007).

Acknowledgements

This work was supported by the European Commission (Marie Curie Fellowship to J.M.C.-S.), and by the Engineering and Physical Sciences Research Council (EPSRC) through grant number EP/I028501/1 and a studentship to C.M.R. funded via the Bristol Chemical Synthesis Doctoral Training Centre (EP/G036764/1). PeakForce AFM was carried out in the Chemical Imaging Facility, University of Bristol, with equipment funded by the Engineering and Physical Sciences Research Council under grant 'Atoms to Applications' grant ref. (EP/K035746/1).

Author information

Authors and Affiliations

1. **School of Chemistry, University of Bristol, Cantock's Close, Bristol, BS8 1TS, UK**

Tiddo J. Mooibroek, Juan M. Casas-Solvas, Robert L. Harniman, Charles M. Renney, Tom S. Carter, Matthew P. Crump & Anthony P. Davis

2. **Department of Chemistry and Physics, University of Almería, Carretera de Sacramento s/n, Almería, 04120, Spain**

Juan M. Casas-Solvas

Contributions

J.M.C.-S. and T.J.M. performed the synthetic work. T.J.M. performed NMR and ITC binding studies, C.M.R. performed some ITC studies and T.S.C. performed the ICD measurements. T.J.M. and M.P.C. were responsible for the structural NMR work. T.J.M. and R.L.H. performed the AFM analyses. The paper was written by T.J.M. and A.P.D. with input from the other authors. A.P.D. designed the receptor and directed the study.

Ethics declarations

Competing interests

The authors declare no competing financial interests.

Supplementary information

Supplementary information

Supplementary information (PDF 8285 kb)